Progress In Electromagnetics Research C, Vol. 21, 45–58, 2011

MINIATURIZED MULTILAYER FOLDED SUBSTRATE INTEGRATED WAVEGUIDE BUTLER MATRIX

Y. J. Cheng, C. A. Zhang, and Y. Fan

EHF Key Lab of Fundamental Science
School of Electronic Engineering
University of Electronic Science and Technology of China
Xiyuan Road 2006, Chengdu 611731, P. R. China

Abstract—Recently, substrate integrated waveguide (SIW) technology attracts more and more attention in the development of millimeter-wave integrated beamforming network (BFN) depending on its inherent advantages. However, the SIW-based BFN usually has a large circuit size. To overcome this weakness, we propose a novel multi-folded SIW Butler matrix at the center frequency of 60 GHz. Two different full-wave simulation tools are employed to validate our design. This folded BFN offers a number of benefits, such as highly compact configuration, low coupling between adjacent paths, and wide operation bandwidth. For convenient use, the SIW ports can be converted to the microstrip line ports arranged in order through a special broadband two-layer transition network. Such a miniaturized SIW Butler matrix can reduce the circuit area by more than 60% compared with the conventional single-layer version.

1. INTRODUCTION

As a very promising technology, substrate integrated waveguide (SIW) attracts more and more attention since its inception [1–12]. This scheme combines the excellent features of both planar transmission lines and conventional metallic waveguide. It also offers a low-cost fabrication technique for mass-production. In addition, the SIW circuits can avoid high radiation loss and parasitic cross-coupling that restrict the development and application of conventional planar integrated beamforming networks (BFNs) and multibeam antenna in

Received 5 February 2011, Accepted 8 April 2011, Scheduled 12 April 2011
Corresponding author: Yu Jian Cheng (yjcheng@emfield.org).

high frequency. As such, the SIW technology is a good choice in the design of millimeter-wave, up-millimeter-wave even terahertz BFNs. Although SIW BFNs possess a number of advantages, their practical use will be limited if the miniaturization is beyond our grasp. There is an overpowering need to develop the miniaturized SIW BFN.

As one of the most popular BFN, Butler matrix usually has complicated configuration and large circuit area. The conventional SIW-based Butler matrix [13–15] consists of several 3 dB couplers, crossings and fixed phase shifters, thus it is very difficult to be miniaturized in the single-layer format. Recently, researchers developed a two-layer Butler matrix to reduce circuit area [16], but there is still room for much improvement.

In this paper, a novel multi-folded SIW Butler matrix is proposed and designed. Firstly, the couplers and layer-to-layer transitions are proposed or modified proper to the multilayer design. Then a four-layer 4×4 BFN is constructed and simulated. LTCC process can be employed in the circuit fabrication. For convenient use, a broadband transition is developed between SIWs in different layers and microstrip lines on the same layer. Simulated results demonstrate that this highly compact structure offers good beamforming performance.

2. DESIGN PROCESS

In this paper, the miniaturized SIW Butler matrix is proposed to operate at the center frequency of 60 GHz. The relative dielectric constant of the LTCC material is 5.7, and its loss tangent is 0.002. The conductor thickness is 0.015 mm, and the dielectric layer thickness per layer is 0.094 mm. The SIW is built by three substrates, thus the height of SIW is 0.282 mm, width of SIW 2 mm, the diameter of metallic via 0.4 mm, and the spacing between adjacent metallic vias 0.6 mm. The basic Butler matrix consists of alternate rows of hybrid junctions and fixed phase shifters, with a typical diagram as shown in Fig. 1 for a 4-element matrix. Excited at one input port, four equal amplitude signals are formed at four output ports with a desired distribution of phase coefficients. Four 3 dB directional couplers, one crossing and two fixed phase shifters should be used in such single-layer architecture.

This conventional configuration can be folded thrice as shown in Fig. 1. The first two 3 dB H-plane couplers (coupler 1) are overlapped at adjacent layers (layer I, II). Their four input ports are also the input ports of Butler matrix (ports $1 \sim 4$). Then, the output ports (a, b) of the bottom coupler are connected to the top layer IV through 1-to-4 transitions, while the center layers (layer II, III) are connected by 1-to-2 slot transitions. The fixed phase shifters are positioned in two top

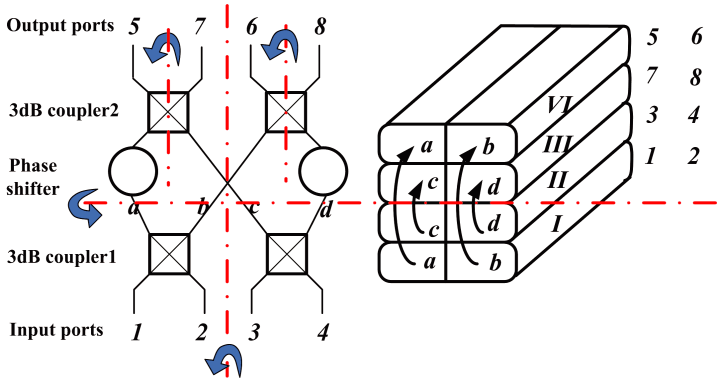

Figure 1. Sketch diagrams of the conventional Butler matrix and the proposed highly compact SIW four-layer Butler matrix.

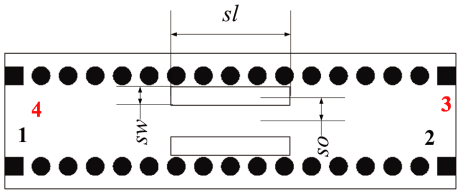

Figure 2. Configuration of the proposed double-slot SIW E-plane coupler.

layers (layer III, IV). After that, two 3 dB E-plane couplers (coupler 2) are used between layers III and IV. Their four output ports are the output ports of Butler matrix (ports 5 $\sim$ 8) as well. This ingenious highly compact layout has another advantage, i.e., no crossing, which avoids additional loss, cross coupling, and mismatch.

2.1. *E*-plane Coupler

To achieve the self-folded of directional coupler, a double-slot E-plane coupler is employed in this design, which has the configuration as shown in Fig. 2. Ports 1 and 2 are located in one layer, while ports 3 and 4 are in the other layer. A pair of long slots is cut on the broadside conductor layer near the metallic via wall. The slot length, sl, slot width, sw, and slot offset, so, are three main parameters to control the coupling constant and optimize the reflection. In this design, $sl = 2.645$ mm, $sw = 0.4$ mm, and $so = 0.55$ mm.

Within the coupling region, there are two kinds of modes, namely TE_{10} mode in SIW and TEM mode in rectangular coaxial line. The initial length of the coupling region, sl, can be determined on the basis of even- and odd-mode theory [17]. There are

$$(\beta_1 - \beta_2) \times sl = \pi/2 \tag{1}$$

In (1), β_1 and β_2 are the phase constants of TE_{10} mode and TEM mode, respectively. They can be determined by simulation tools.

The simulated results of the proposed double-slot SIW E-plane coupler are shown in Fig. 3. The reflection and coupling are below -28 dB within the frequency band of $55 \sim 65$ GHz. It also has well-balanced outputs. The phase difference between output ports, i.e., $\angle S_{31}$–$\angle S_{21}$, is $90.25^\circ \pm 0.5^\circ$ within the interested frequency band.

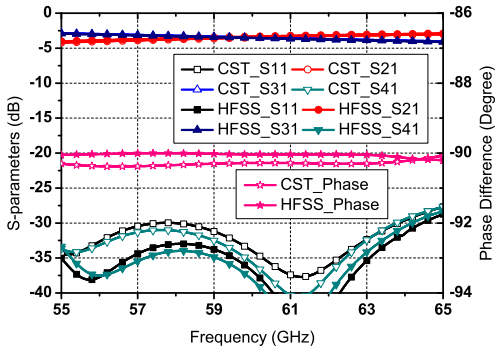

Figure 3. S-parameters of the proposed double-slot SIW E-plane coupler.

2.2. H-plane Coupler

Two different SIW couplers are used in this design to simplify the multilayer structure. One is the above E-plane coupler, and the other is an H-plane coupler, which has a continuous coupling aperture to achieve the strong coupling.

The even- and odd-mode theory is also employed in the design [17]. There are two modes propagated within the coupling section, i.e., TE_{10} and TE_{20} in SIW. Their phase constants are β_1 and β_2, respectively. Thus, a similar equation can be used to calculate the required length of coupling section, la.

$$(\beta_1 - \beta_2) \times la = \pi/2 \tag{2}$$

Waveguide steps are used to achieve the good matching. On the other hand, the steps make the final la shorter than the calculated one.

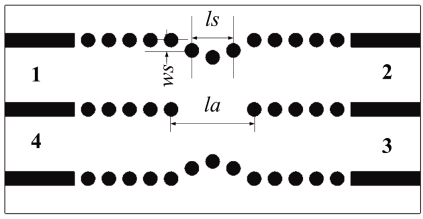

Figure 4. Configuration of the proposed SIW H-plane coupler.

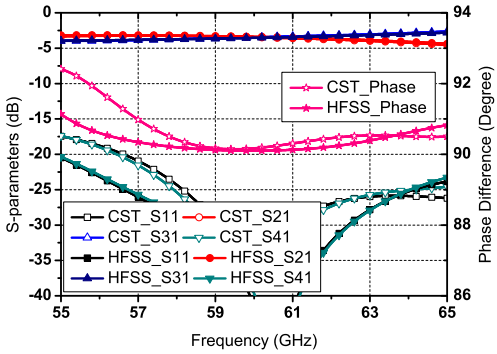

Figure 5. S-parameters of the proposed SIW H-plane coupler.

The configuration of the proposed structure is shown in Fig. 4 and the simulated results are shown in Fig. 5. The corresponding parameters are: $la = 2.4\,\text{mm}$, $ls = 1.2\,\text{mm}$, and $ws = 0.5\,\text{mm}$. The reflection and coupling are almost below $-20\,\text{dB}$ within the frequency band of $55 \sim 65\,\text{GHz}$. It also has well-balanced outputs. The phase difference between output ports, $\angle S_{31} - \angle S_{21}$, is $90.5^\circ \pm 1^\circ$ within the frequency band of $57 \sim 65\,\text{GHz}$.

2.3. Layer-to-Layer Transition

To provide size reduction, the SIW Butler matrix is folded and distributed in different layers. Therefore, different layer-to-layer transitions are necessary in this design to connect SIWs in different layers. One is the backward 1-to-2 transition, and the other is the backward 1-to-4 transition.

For the 1-to-2 one, a transverse slot is cut on the middle broadside to couple energy between two neighboring SIWs as shown in Fig. 6. The design of 1-to-4 transition, which couples energy from layer I to layer IV, is more difficult. Three 1-to-2 transitions can be grouped as a

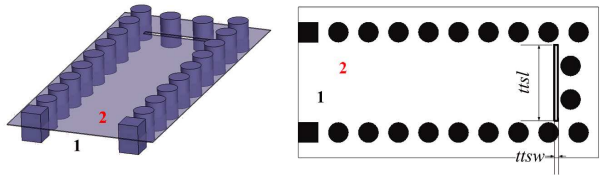

Figure 6. Configuration of the proposed SIW 1-to-2 transition.

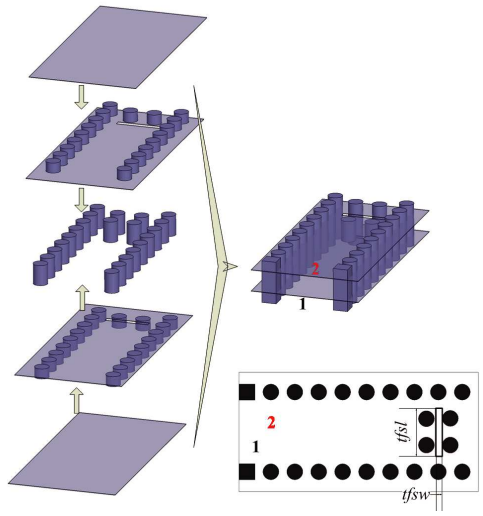

Figure 7. Configuration of the proposed SIW 1-to-4 transition.

1-to-4 transition. To simplify the topology and reduce the transmission loss, a novel 1-to-4 structure is developed in this design as shown in Fig. 7. Two transverse slots are cut in different conductor layers, while two additional metallic posts are inserted into middle dielectric layers.

In these figures, $ttsl = 1.51\,\text{mm}$, $ttsw = 0.1\,\text{mm}$, $tfsl = 1.19\,\text{mm}$, and $tfsw = 0.15\,\text{mm}$. The simulated reflection of 1-to-2 transition is below $-30\,\text{dB}$ within the frequency band of $55 \sim 65\,\text{GHz}$, while the simulated reflection of 1-to-4 transition is almost below $-20\,\text{dB}$ within the frequency band of $56 \sim 63\,\text{GHz}$ as shown in Fig. 8. Such two transitions provide excellent performance over a wide bandwidth.

2.4. Whole Configuration

Now, the SIW four-layer Butler matrix can be constructed by two H-plane couplers, two E-plane couplers, two 1-to-2 transitions, two 1-

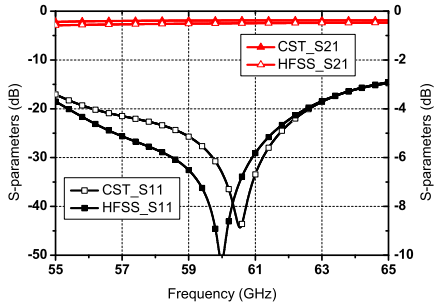

Figure 8. *S*-parameters of the proposed SIW 1-to-4 transition.

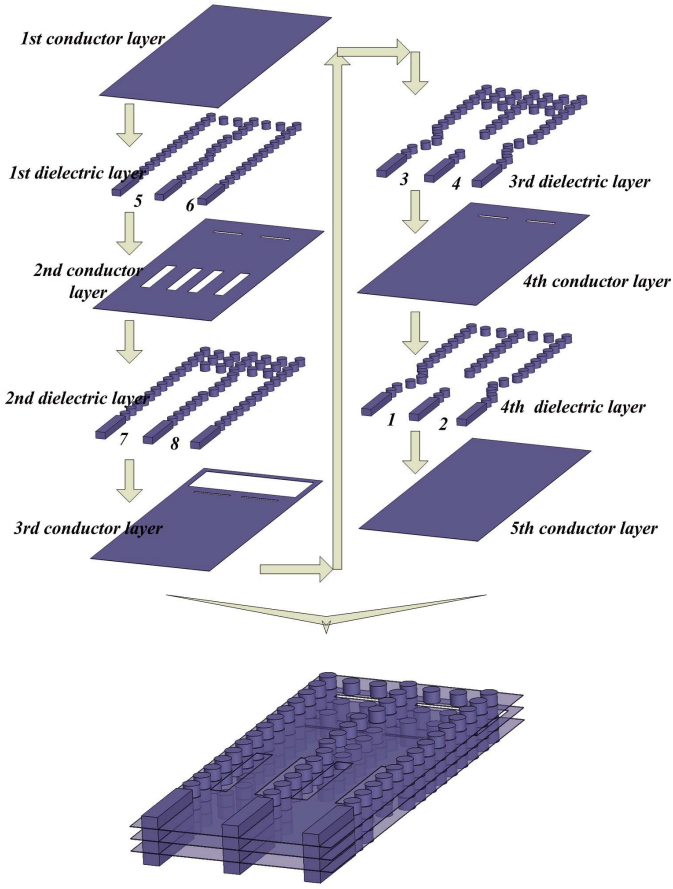

Figure 9. Configuration of the proposed miniaturized SIW butler matrix.

to-4 transitions, and two fixed phase shifters. Its 3D configuration and dimension are shown in Figs. 9, 10 respectively. Here, $pl_1 = 1.8\,\text{mm}$, $pw_1 = 0.187\,\text{mm}$, $ph_2 = 1.8\,\text{mm}$, $pw_2 = 0.2\,\text{mm}$.

In this design, the equal-length unequal-width phase shifters are employed to achieve the required phase shift with compact size [18]. As is well known, the SIW has a width-dependent propagation constant. Therefore, the phase shift can be achieved with an equal SIW length through the use of non-uniform widths. Since the SIW is synthesized in a planar substrate with arrays of metallic via, this feature can easily be deployed to realize the required phase shift by adjusting the position of vias to form variable SIW widths.

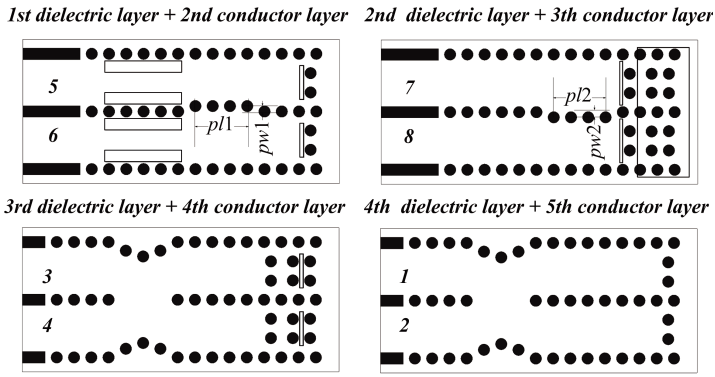

Figure 10. Dimension of the proposed miniaturized SIW Butler matrix.

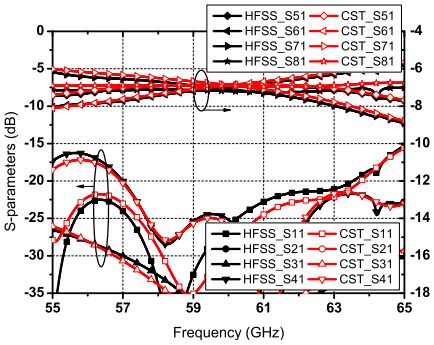

Figure 11. S-parameters excited at port 1 of the proposed miniaturized SIW Butler matrix.

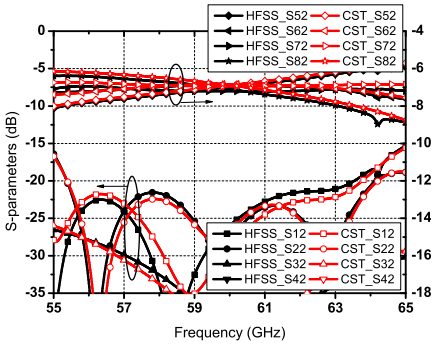

Figure 12. S-parameters excited at port 2 of the proposed miniaturized SIW Butler matrix.

3. SIMULATED RESULTS

3.1. Basic Butler Matrix

Now, the whole structure is modeled and simulated by two full-wave simulators CST and HFSS, respectively. The results implemented by different simulators are very similar as shown in Figs. 11–13. The return losses and the coupling coefficients are simulated from 55 GHz to 65 GHz. For port 1 at the center frequency 60 GHz, all coefficients are below −25 dB. Excited at port 2, S_{12}–S_{42} are all less than −27 dB at the center frequency 60 GHz. The transmissions S_{51}–S_{81} and S_{52}–S_{82} are observed with the low amplitude ripples. From 55 GHz to 63 GHz, ±1 dB amplitude ripples can be achieved. Fig. 13 shows the simulated

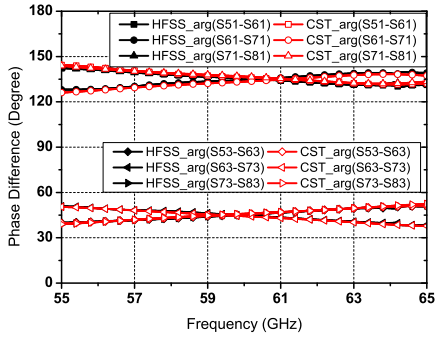

Figure 13. Phase differences excited at ports 1 and 3 of the proposed miniaturized multilayer folded SIW Butler matrix.

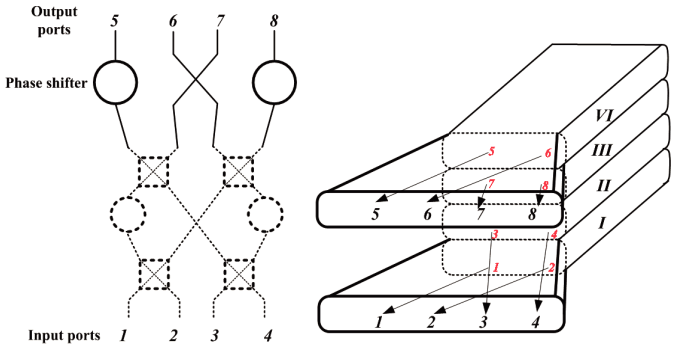

Figure 14. Sketch diagram of the proposed multilayer Butler matrix with transition network. (Dashed part is the actualized basic Butler matrix).

results for phase differences excited from ports 1 and 3. It is clear that the phase ripple is also low and this BFN can offer a series of four phase coefficients, approximate 135°, 45°, −45° and −135°. ±5° phase bandwidth are 57 ∼ 65 GHz for port 1 and 55.5 ∼ 63.5 GHz for port 3, respectively. Similar results can be found when excited at other input ports. The simulation results validate the correct of our design and verify this configuration has good amplitude and phase performance over a wideband.

3.2. Folded Butler Matrix with Transition Network

For convenient use, the input SIWs or output SIWs of the proposed multilayer structure distributed in different layers will be converted to microstrip lines etched on the same conductor layer. Moreover, the output and input ports should be arranged in order. Thus, a proper SIW transition network should be developed to finish such a conversion task.

The actualized folded Butler matrix with transition network has the sketch diagram as shown in Fig. 14. The input ports 3 and 4

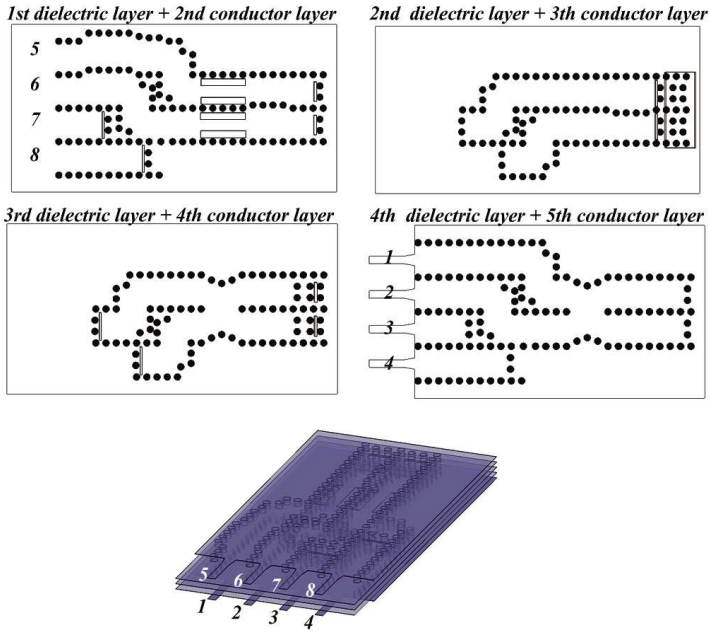

Figure 15. Configuration of the proposed miniaturized folded SIW Butler matrix with transition network.

in layer II and output ports 7 and 8 in layer III are transferred to the top and bottom layers (layer I and IV), respectively. Due to the multilayer configuration, such a transition network is much simpler compared with the conventional one and avoid the use of crossing, which is indispensable in the design of conventional Butler matrix as shown in Fig. 14. Some forward 1-to-2 layer transitions (the slot length is 1.6 mm and the slot width is 0.1 mm) are used, which have the similar configuration as shown in Fig. 6. The difference is that the input and output ports are positioned at the same side of different layers for the backward one while positioned at the opposite sides of different layers for the forward one. Some unequal-width phase shifters are used to compensate the phase shift generated by unequal paths of the transition network.

After full-wave simulation and optimization, the finally configuration of the proposed SIW multilayer Butler matrix with transition network are shown in Fig. 15. Certainly, the transition network can be folded above the layer VI and below layer I to miniaturize the circuit size more.

The simulated results implemented by HFSS with an excitation at port 1 are shown in Fig. 16. The simulated return losses and the coupling coefficients are below −15 dB from 57 GHz to 65 GHz. From 57 GHz to 63 GHz, ±1 dB amplitude ripples can be achieved. Excited at other input ports, similar results can be found. Fig. 17 shows the simulated results for phase differences excited from ports 1 and 3. ±5° phase bandwidth are 58 ∼ 64.2 GHz for port 1 and 56.2 ∼ 63.4 GHz for port 3. Good performances are observed within the operation frequency band.

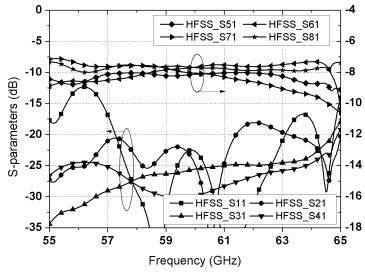

Figure 16. *S*-parameters excited at port 1 of the proposed miniaturized SIW Butler matrix with transition network.

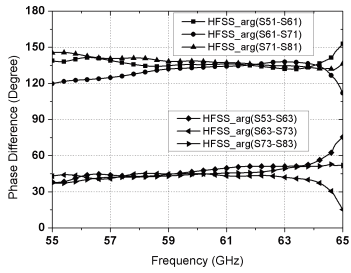

Figure 17. Phase differences excited at ports 1 and 3 of the proposed miniaturized SIW Butler matrix with transition network.

Table 1. Comparison for the proposed folded SIW Butler matrix with transition network to the conventional single-layer one.

		Our work			
Size	Length	14.4 mm			
	Width	8.5 mm			
Amplitude		Port5	Port6	Port7	Port8
	58 GHz	1.00	0.98	1.06	1.06
	60 GHz	1.00	1.05	1.01	1.05
	62 GHz	1.00	1.05	0.94	1.02
Phase		S_{51}–S_{61}	S_{61}–S_{71}	S_{71}–S_{81}	
	58 GHz	135.06	128.47	141.02	
	60 GHz	135.50	133.02	138.47	
	62 GHz	134.50	135.73	135.77	
		Single-layer structure in [15]			
Size	Length	21.5 mm			
	Width	14.2 mm			
Amplitude		Port5	Port6	Port7	Port8
	58 GHz	1.00	0.97	1.08	0.99
	60 GHz	1.00	1.04	1.17	1.08
	62 GHz	1.00	0.99	1.26	1.06
Phase		S_{51}–S_{61}	S_{61}–S_{71}	S_{71}–S_{81}	
	58 GHz	117.64	144.00	136.88	
	60 GHz	124.67	134.22	141.33	
	62 GHz	132.78	132.24	138.70	

The simulated results of the proposed miniaturized Butler matrix with transition network is compared with that of the conventional single-layer configuration in [15]. They are excited at the same port with the same relative permittivity. As shown in Table 1, this folded Butler matrix not only reduces the circuit area much more, but also improves the phase characteristics.

4. CONCLUSION

In this paper, the conventional single-layer SIW-based Butler matrix is folded thrice to construct a miniaturized four-layer structure. This work provides an efficient method to reduce the circuit area of SIW Butler matrix and not to worsen its excellent characteristics. After proper selection and design sub-components, a 60 GHz prototype has

been designed and simulated. Then, a wideband transition network is developed to transfer the SIW input ports (or output ports) in different dielectric layers to the microstrip line ports arranged in order etched on the same conductor layer. It not only has relative simple architecture because of the multilayer layout, but also has the good beamforming ability over a wide bandwidth. But compared with the single-layer conventional circuit, this type of folded SIW Butler matrix may increase the complexity in fabrication processes.

ACKNOWLEDGMENT

This work is supported by the National Natural Science Foundation of China (NSFC) under grant 61001028.

REFERENCES

1. Lo, Y. T. and S. W. Lee, *Antenna Handbook*, Van Nostrand Reinhold, New York, 1993.
2. Hirokawa, J. and M. Ando, "Efficiency of 76-GHz post-wall waveguide-fed parallel-plate slot arrays," *IEEE Trans. Antennas Propag.*, Vol. 48, No. 11, 1742–1745, 2000.
3. Che, W., E. K. N. Yung, K. Wu, and X. Nie, "Design investigation on millimeter-wave ferrite phase shifter in substrate integrated waveguide," *Progress In Electromagnetics Research*, Vol. 45, 263–275, 2004.
4. Grigoropoulos, N. and P. R. Young, "Compact folded waveguides," *34th Eur. Microw. Conf.*, 973–976, Amsterdam, Netherlands, 2004.
5. Sanz Izqueirdo, B., N. Grigoropoulos, and P. R. Young, "Ultra-wideband multilayer substrate integrated folded waveguides," *IEEE MTT-S Digest*, 610–612, 2006.
6. Grigoropoulos, N., B. Sanz Izquierdo, and P. R. Young, "Substrate integrated folded waveguide (SIFW) and filters," *IEEE Microw. Wireless Compon. Lett.*, Vol. 15, No. 12, 829–831, 2005.
7. Zhang, X. C., Z. Y. Yu, and J. Xu, "Novel band-pass substrate integrated waveguide (SIW) filter based on complementary split ring resonators," *Progress In Electromagnetics Research*, Vol. 72, 39–46, 2007.
8. Wang, R., L. S. Wu, and X. L. Zhou, "Compact folded substrate integrated waveguide cavities and bandpass filter," *Progress In Electromagnetics Research*, Vol. 84, 135–147, 2008.

9. Ismail, A., M. S. Razalli, M. A. Mahdi, R. S. A. Raja Abdullah, N. K. Noordin, and M. F. A. Rasid, "X-band trisection substrate-integrated waveguide quasi-elliptic filter," *Progress In Electromagnetics Research*, Vol. 85, 133–145, 2008.
10. Hong, W., K. Wu, H. J. Tang, J. X. Chen, P. Chen, Y. J. Cheng, and J. F. Xu, "SIW-liked guided wave structure and application," *IEICE Trans. Electronics*, Vol. 92, No. 9, 1111–1123, 2009.
11. Wu, L.-S., J.-F. Mao, W. Shen, and W.-Y. Yin, "Extended doublet bandpass filters implemented with microstrip resonator and full-/half-mode substrate integrated cavities," *Progress In Electromagnetics Research*, Vol. 108, 433–447, 2010.
12. Bakhtafrooz, A., A. Borji, D. Busuioc, and S. Safavi-Naeini, "Novel two-layer millimeter-wave slot array antennas based on substrate integrated waveguides," *Progress In Electromagnetics Research*, Vol. 109, 475–491, 2010.
13. Yamamoto, S., J. Hirokawa, and M. Ando, "A beam switching slot array with a 4-way Butler matrix installed in a single layer post-wall waveguide," *IEEE International Symposium on Antennas and Propagation*, Vol. 1, 138–141, 2002.
14. Chen, P., W. Hong, Z. Q. Kuai, and H. M. Wang, "A multibeam antenna based on substrate integrated waveguide technology for MIMO wireless communications," *IEEE Trans. Antennas Propag.*, Vol. 57, No. 6, 1813–1821, 2009.
15. Chen, C. J. and T. H. Chu, "Design of a 60-GHz substrate integrated waveguide Butler matrix — A systematic approach," *IEEE Trans. Microw. Theory Tech.*, Vol. 58, No. 7, 1724–1733, 2010.
16. Ali, A., N. J. G. Fonseca, F. Coccetti, and H. Aubert, "Design and implementation of two-layer compact wideband Butler matrices in SIW technology for Ku-band applications," *IEEE Trans. Antennas Propag.*, Vol. 59, No. 2, 503–512, 2011.
17. Liu, H., *Microwave Network and Applications*, Publishing Company of UESTC, Chengdu, 1989
18. Cheng, Y. J., W. Hong, and K. Wu, "Millimetre-wave monopulse antenna incorporating substrate integrated waveguide phase shifter," *IET Microw. Antennas Propag.*, Vol. 2, No. 1, 48–52, 2008.